

# Electrochemically Nanostructured ZnSe for Photonic and Optoelectronic Applications

I.M. TIGINYANU<sup>1,2</sup>, E. MONAICO<sup>2</sup>, V.V. URSAKI<sup>3</sup>, G. COLIBABA<sup>4</sup>, D.D. NEDEOGLO<sup>4</sup>,  
N. LEPORDA<sup>1</sup>

<sup>1</sup>Institute of Electronic Engineering and Industrial Technologies, Academy of Sciences of Moldova, MD-2028, Chisinau, Moldova

<sup>2</sup>National Center for Materials Study and Testing, Technical University of Moldova

<sup>3</sup>Institute of Applied Physics, Academy of Sciences of Moldova, MD-2028 Chisinau, Moldova

<sup>4</sup>State University of Moldova, Mateevich str. 60, Chisinau MD-2009, Moldova

**Abstract** — In this paper we demonstrate the possibility to control the conductivity of ZnSe in a degree acceptable for electrochemical nanostructuring. Technological methods for the preparation of nanostructures and composite materials suitable for photonic and optoelectronic applications are developed.

## I. INTRODUCTION

While the electrochemical etching is a versatile tool for use in nanostructuring of narrow and medium band-gap materials such as Si, InP, GaAs, GaP, ZnTe and CdSe, the use of this method for wide bandgap II-VI semiconductors is still a challenge. The related difficulties are linked with controlling the conductivity of the source material, as high carrier concentration is needed to apply anodic etching for nanostructuring. It is difficult to obtain wide bandgap semiconductors with high conductivity due to self-compensation phenomena inherent to these materials [1].

Development of a reliable technology for controllable doping of the semiconductor material is a first imperative step towards controlled electrochemical nanostructuring. Doping crystals with III-group elements proved to be an effective way of solving this problem with ZnSe [2,3]. The possibility to control the conductivity of ZnSe crystals by doping the samples with Al from a Zn+Al melt was demonstrated [4,5,6]. This procedure allows producing suitable samples for controlled nanostructuring using electrochemical etching techniques.

The goal of this paper is to demonstrate the possibility to control the conductivity of ZnSe in a degree acceptable for electrochemical nanostructuring, and for the preparation of nanostructures and composite materials suitable for photonic and optoelectronic applications.

## II. TECHNOLOGICAL METHODS FOR THE CONTROL OF ZNSE CONDUCTIVITY

The Al doping of as-grown high resistivity ( $\rho \approx 10^8 \Omega\cdot\text{cm}$ ) n-ZnSe single crystals grown from a melt was carried out by means of high temperature (950°C) annealing in a Zn+Al melt with different doping impurity contents during 100 hours. The doping level was controlled by the variation of the Al content X in the melt [(100 - X) at.% Zn + X at.% Al], with X varied in the range from 0.1

to 40 at.%. The influence of the annealing in Zn+Al melt upon electrical parameters of ZnSe crystals is summarized in Table 1. The analysis of data in Table 1 is indicative of a rather complicated dependence of the electrical parameters of ZnSe crystals upon the concentration of Al in the Zn+Al melt. The mechanisms responsible for the variation of electrical parameters as a function of annealing conditions were discussed elsewhere [4]. According to the results of electrical characterization [4], the increase of the Al concentration can be divided in four intervals as follows: (i) from 0 to 0.5 at. %; (ii) from 0.5 to 5 at. %; (iii) from 5 to 20 at. %; (iv) more than 20 at. %. The enhancement of Al content in the melt within the first and third intervals leads to the increase of the electron concentration in crystals, while the increase of the Al concentration within the second and fourth intervals results in the decrease of the electron concentration. This non-monotonous behavior is explained by complex processes of interaction between the doping impurity and the intrinsic defects or residual impurities. The dynamics of the formation and dissociation of associative centers determines the complex character of the dependence of electrical parameters upon the density of Al doping impurity.

TABLE I. ELECTRICAL PARAMETERS OF N-ZNSE:ZN+X AT.% AL SINGLE CRYSTALS AND THE MEAN PORE DIAMETER OF POROUS SAMPLES PRODUCED BY ANODIZATION

X at.% Al	n, cm <sup>-3</sup>	$\sigma$ , $\Omega^{-1}\text{cm}^{-1}$	R $\sigma$ , cm <sup>2</sup> /V·s	Mean pore diameter, nm	Required anodization voltage, V
0	$7.2 \cdot 10^{16}$	1.49	130	400-500	>30
0.1	$9.3 \cdot 10^{16}$	3.15	210	200-300	>20
0.3	$3.0 \cdot 10^{17}$	12.64	265	100	>9
0.5	$2.1 \cdot 10^{18}$	29.30	126	40	>6
1	$9.1 \cdot 10^{17}$	12.77	88	40	>6
5	$5.8 \cdot 10^{17}$	17.22	186	60	>8
10	$5.1 \cdot 10^{17}$	15.03	184	60	>8
20	$1.7 \cdot 10^{18}$	20.10	72	40	>6
40	$4.4 \cdot 10^{16}$	1.07	155	600-900	>50

## III. ELECTROCHEMICAL NANOSTRUCTURING

The anodic etching was carried out in  $K_2Cr_2O_7:H_2SO_4:H_2O$  electrolyte with the ratio of 5:100:10 at 25 °C in potentiostatic regime with applied voltage varied. The morphology parameters of the anodized ZnSe samples (the pore mean diameter and the thickness of the skeleton walls) follow the variation of electrical parameters in crystals as summarized in table 1. The anodization of ZnSe samples obtained from a pure Zn melt, i. e. with the electron concentration of  $7.2 \times 10^{16} \text{ cm}^{-3}$ , requires voltages over 30 V for the formation of porous structure and the resulted pores have the mean diameter as high as 400 - 500 nm, as illustrated in Fig. 1a for a sample anodized at 40 V. The increase of the electron concentration to  $(1-2) \times 10^{18} \text{ cm}^{-3}$  in samples allows one to reduce the anodization voltage down to 6 V and to obtain porous structures with the pore mean diameter of about 40 nm as shown in Fig. 1b for a sample with electron concentration of  $9 \times 10^{17} \text{ cm}^{-3}$  produced by annealing in a Zn+Al melt with 1 at % of Al.

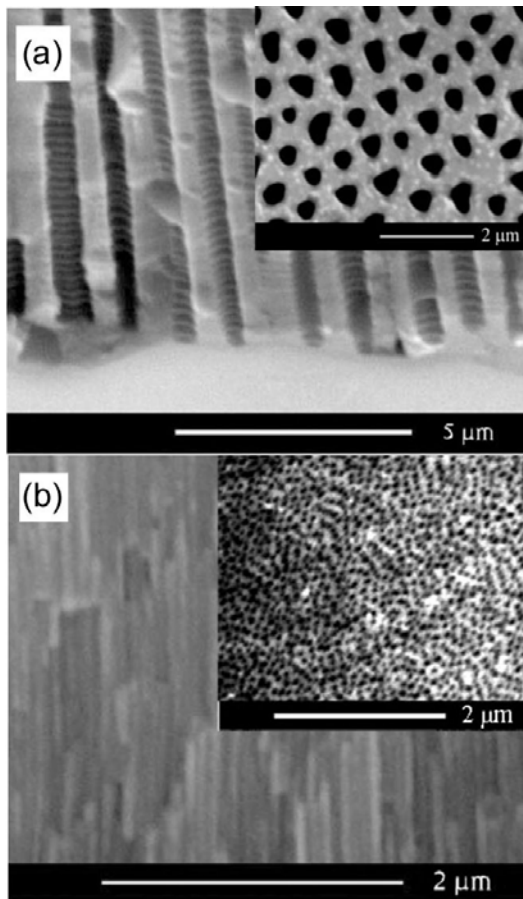


Fig. 1. SEM image taken in cross section from porous ZnSe samples produced by anodic etching of crystals annealed in a pure Zn melt (a), and annealed in a Zn+Al melt with the concentration of Al equal to 1 at % (b). Inserted is the top view.

One should mention that the variation of the electron concentration from around  $1 \times 10^{18} \text{ cm}^{-3}$  to  $2 \times 10^{18} \text{ cm}^{-3}$  does not change significantly the morphology of the anodized samples. Therefore, the morphology of samples produced by anodization of ZnSe crystals annealed in Zn+Al melt

with 0.5, 1, and 20 at % of Al is similar to that illustrated in Fig. 1b, i. e. the morphology of the anodized samples is not determined by the concentration of Al impurity in the melt, but by the produced electron concentration in crystals. The increase of electron concentration in crystals from  $7 \times 10^{16}$  to  $(1-2) \times 10^{18} \text{ cm}^{-3}$  allows one to reduce the pore diameter from 400 - 500 nm to 40 nm. The width of the porous skeleton walls correlates with the diameter of pores, i.e. in all porous samples the width of the skeleton walls proves to be nearly equal to the pore diameter.

The possibility to control the diameter of pores just by changing the applied potential during anodic etching allows one to prepare multilayer porous structures in one technological process. Fig. 2a shows an example of a porous structure that consists of three layers exhibiting pores with different transverse dimensions: the average diameter is 500 nm, 200 nm and 60 nm for the upper, middle and lower layer, respectively. As evidenced by EDX analysis, the porous skeleton in the whole porous structure is characterized by stoichiometric composition inherent to the ZnSe compound. It is interesting to note that the morphology of the multilayer porous structure does not depend upon the mode of the transition from one value of the applied voltage to another one: it can be both sharp and with a temporary cease of the anodic etching. This is quite different from the case of n-InP where consecutive on-off switching of the etching process leads to the alternation of porous layers exhibiting by turns crystallographically oriented and current-line oriented pores [7].

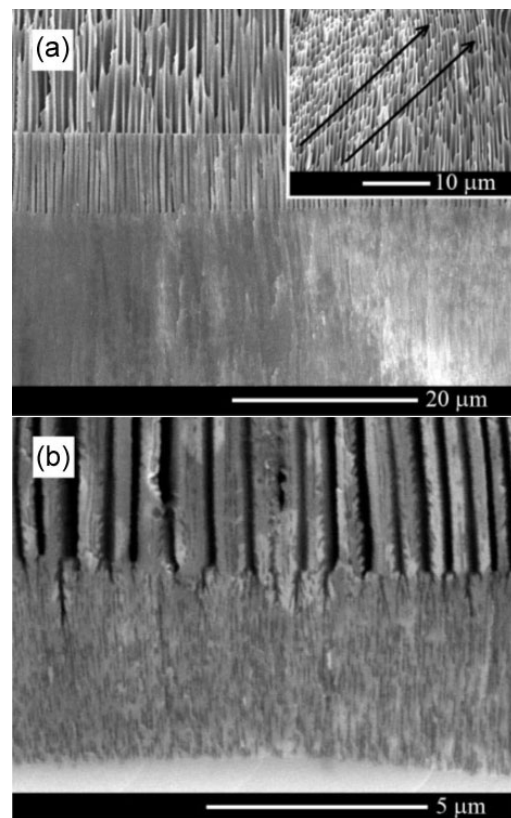


Fig. 2. SEM images taken from multilayer porous structures in cross-section: three layers (a) and two layers (b). The insert shows the alignment of pore rows along the  $\langle 110 \rangle$  crystallographic direction in ZnSe.

Successive anodization of ZnSe substrates at varied applied voltage results in layer porosification at different length scales. The approach is demonstrated by the image presented in Fig. 2b, the sample being subjected to anodic etching in two steps at applied voltages of 15 V and 8 V, respectively. The first anodization step results in the formation of a porous layer with the transverse dimensions of pores and pore walls as high as several hundreds of nanometers (see the upper porous layer in Fig. 2b). The second anodization step has a double function: first, it leads to the formation of a new porous layer with pores of about 60 nm in diameter (see the lower porous layer in Fig. 2b) and, second, it simultaneously generates similar pores in the thick walls of the upper porous layer. The observed successive porosification of the same layer at two different length scales opens new possibilities for the design and fabrication of device structures based on porous semiconductor compounds. Note that a similar type of successive porosification at two length scales was applied recently to macroporous Si by Lehmann [8].

#### IV. ZnSE STRUCTURES WITH PORES PARALLEL TO THE SURFACE OF THE SUBSTRATE

Porous ZnSe structures with pores propagating in the direction parallel to the sample surface (Fig. 3) are of especial interest for the fabrication of two-dimensional and three-dimensional photonic crystals including metallo-dielectric ones, since this geometry allows a wide implementation of structures due to the large surface of samples as compared to the geometry with pores propagating perpendicularly to the surface.

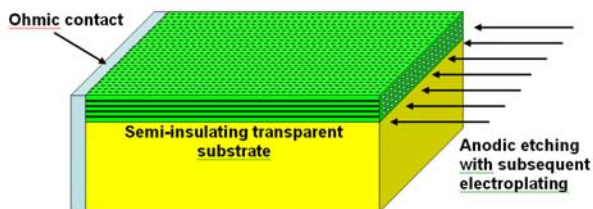


Fig. 3. A schematic representation of the technology for the preparation of ZnSe templates with pores propagating in the direction parallel to the sample surface.

The investigations demonstrated that in the geometry illustrated in Fig.3 the porous layer is formed at the periphery of the sample, i. e. near the cleavage. Since the porous layer is fragile, it is inconvenient to work with such samples. A possibility to avoid this drawback was explored through the electrochemical etching using a photoresist mask. In this geometry the ohmic contact is deposited onto the opposite surface of the sample, and electrochemical etching is performed through a window in the photoresist. The experiments demonstrated that the electrochemical etching starts at the interface between the open surface and the electrolyte. Consequently, due to the high conductivity of the sample, the pores propagate along the current line in all directions, inclusively underneath the fotoresist in a direction parallel to the sample surface, as illustrated in Fig. 4.

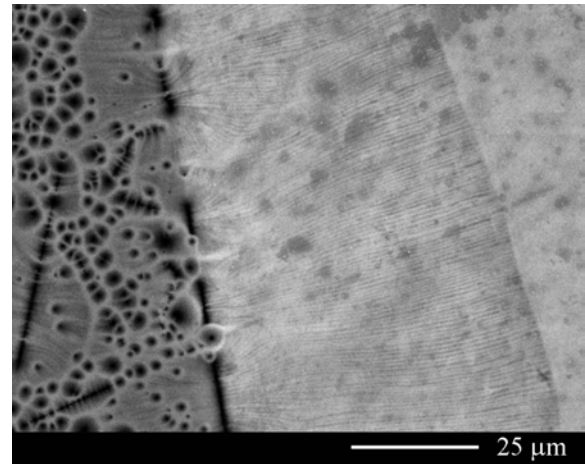


Fig. 4. SEM image of a porous layer with pores propagating under the photoresist layer in a direction parallel to the sample surface and perpendicularly to the line which marks the edge of the photoresist layer.

One should note that an intact layer remains underneath the photoresist with the thickness which correlates with the thickness of the pore walls. Underneath this intact film the porous layer is formed with pores directed parallel to the sample surface. One can see from Fig. 4 that at the beginning of anodization the etching starts at imperfections in the ZnSe substrate near the edge of the photoresist layer. After the initial pitting of the surface, further etching proceeds in all directions, i.e. in the first approximation radially away from the surface imperfection. This process is better illustrated in Fig. 5. As a result, a porous domain forms around each etching pit.

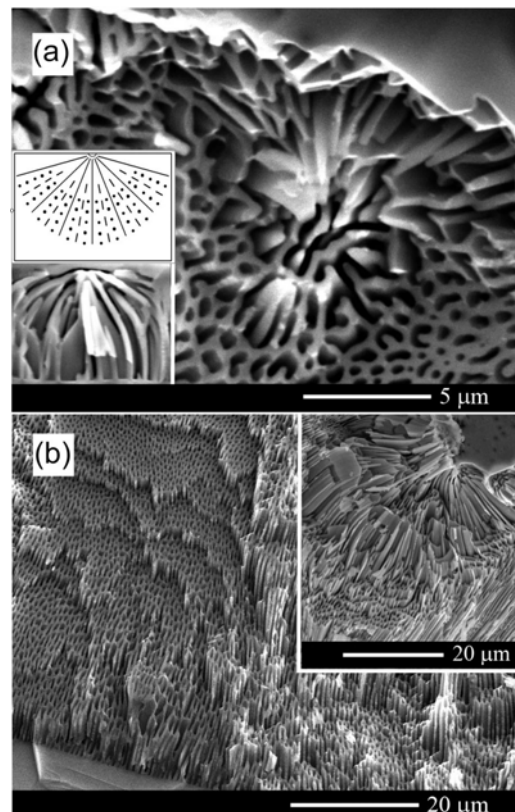


Fig. 5. Development of porous structure in ZnSe.

## V. PREPARATION OF ZnSe-METAL COMPOSITES

The development of nanocomposite materials is a dynamical branch of science and technology, since it opens possibilities for the elaboration of new multifunctional materials combining the properties of the constituents with new properties not inherent to the initial components. A new possibility appears in the case of ordered structures for the exploration of their photonic properties in integrated optics, communication systems etc. The possibility to use a ZnSe porous matrix for the purpose of electroplating arrays of metal nanotubes was demonstrated.

Pt electroplating was carried out in 20  $\mu\text{m}$  thick porous ZnSe layer with diameters of pores of about 400 nm. The electrochemical deposition of Pt was performed at 40 °C for 8 h in a common two-electrode plating cell containing 2 g/l Pt where the porous sample served as working electrode, while a platinum wire was used as counter electrode. A pulsed voltage regime with rectangular pulses was provided by a home-made generator. During the 200  $\mu\text{s}$  pulse time a cathodic potential of  $-40$  V was applied between the two electrodes to electrochemically reduce the metal species on the inner surface of the porous matrix in contact with the electrolyte. After each pulse a delay time as long as 1 s was used at zero external voltage applied to allow ions to diffuse into pore regions depleted during the deposition pulse. Besides, magnetic stirring was applied to provide recovery of the ion concentration in the electrolyte along the whole depth of pores. As one can see from Fig. 6, electrochemical deposition of Pt resulted in the formation of metal nanotubes with the wall thickness of about 50 nm.

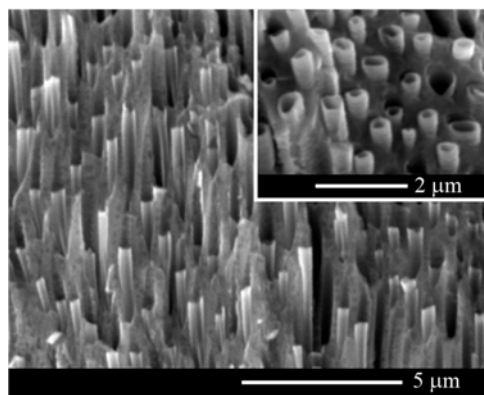


Fig. 6. SEM image taken from cleaved porous n-ZnSe sample after pulsed electrodeposition of Pt. The insert illustrates a top view after the sample was additionally cleaved along a plane nearly perpendicular to the pores.

Pieces of Pt nanotubes getting out from pores are clearly seen in the cross-sectional view taken from a cleaved sample, see insert in Fig. 6. The quality of nanotubes is indicative of good uniformity of metal deposition on the inner surface of pores. The uniformity of Pt deposition as a function of depth was proved also by EDX analysis of chemical composition. The amount of deposited Pt proved to be proportional to the deposition time. Note that in SEM images Pt nanotubes look bright in comparison with the porous n-ZnSe skeleton walls. Like in similar Pt-InP structures [9], this seems to be a consequence of the charging phenomenon caused by the potential barrier at the Pt-ZnSe interface.

## VI. CONCLUSION

The results of this study demonstrate the possibility of preparation of nanostructured ZnSe templates with pores oriented in directions either perpendicular or parallel to the substrate surface. The feasibility of ZnSe-based nanotemplates for nanofabrication is also demonstrated. The high conductivity of the nanotemplate skeleton provides conditions for uniform electrochemical deposition of metal species on the inner surface of pores, resulting in the formation of arrays of metal nanotubes embedded in wide-bandgap semiconductor matrix. These metallo-semiconductor structures are promising for the elaboration of photonic crystals and photonic elements.

## ACKNOWLEDGMENTS

This work was supported by the Supreme Council for Research and Technological Development of the Academy of Sciences of Moldova under grant no 09.836.05.07F.

## REFERENCES

- [1] M.Y. Marfaing. *Prog. Cryst. Growth Charact.* **4**, 317 (1981).
- [2] B. Reinhold and M. Wienecke. 1999 *J. Crystal Growth* **204**, 434 (1999).
- [3] M. Prokesch, K. Irmascher, J. Gebauer and R. Krause-Rehberg. *J. Crystal Growth.* **214/215**, 988 (2000).
- [4] G. N. Ivanova, D. D. Nedeoglo, N. D. Negeoglo, V. P. Sirkeli, I. M. Tiginyanu and V. V. Ursaki. *J. Appl. Phys.* **101**, 063543 (2007).
- [5] E. Monaico, I. M. Tiginyanu, V. V. Ursaki, A. Sarua, M. Kuball, D. D. Nedeoglo and V. P. Sirkeli. *Semicond. Sci. Technol.* **22**, 1115–1121 (2007).
- [6] G. Irmer, E. Monaico, I.M. Tiginyanu, G. Gartner, V.V Ursaki, G. V. Kolibaba and D. D. Nedeoglo. *J. Phys. D: Appl. Phys.* **42**, 045405 (2009).
- [7] M. Christophersen, S. Langa, J. Carstensen, I. M. Tiginyanu, and H. Föll. *Phys. Status Solidi A* **197**, 197-203 (2003).
- [8] V. Lehmann. *Phys. Status Solidi A* **202**, 1365 (2005).
- [9] Ion Tiginyanu, Elena Monaico, Eduard Monaico. *Electrochemistry Communications* **10**, 731–734 (2008).